Supporting Information

Holey Reduced Graphene Oxide-assisted Oxide-derived Bi for Efficient Nitrogen Electroreduction

Peng Huang,[a] Zhuo Cheng,*[b] Liang Zeng,[c] Lulu Tan,[a] Jian Yu,[a] Joshi Rushikesh,[b] Liang-Shih Fan[b] and Yujie Zhu,*[a, d]

[a] School of Chemistry, Beihang University, Beijing 100191, P. R. China

[b] William G. Lowrie Department of Chemical and Biomolecular Engineering, 151 West Woodruff Avenue, Koffolt Laboratories, The Ohio State University, Columbus, OH 43210, United States

[c] Key Laboratory for Green Chemical Technology of Ministry of Education, School of Chemical Engineering and Technology, Collaborative Innovation Center of Chemical Science and Engineering, Tianjin University, Tianjin 300072, P. R. China

[d] Beijing Advanced Innovation Center for Biomedical Engineering, Beihang University, Beijing 100191, P. R. China

* Corresponding authors. Email: cheng.963@osu.edu (Z. C.), yujiezhu@buaa.edu.cn (Y. Z.)

Chemicals and materials: Sulfuric acid (H_2SO_4, 95%~98%), potassium chloride (KCl, ≥99.5%), hydrochloric acid (HCl, 36%~38%), and ethyl alcohol (C_2H_5OH, ≥99.8%) were purchased from Beijing Chemical Works. sodium hydroxide (NaOH, 98%), salicylic acid ($C_7H_6O_3$, 99%), trisodium citrate dihydrate ($Na_3C_6H_5O_7 \cdot 2H_2O$, 99%), sodium hypochlorite solution (NaClO, available chlorine 11%~14%), sulfanilic acid ($C_6H_7NO_3S$, ACS, 98-102%), and acetic acid (CH_3COOH, 99%) are obtained from Alfa Aesar. Hydrazine hydrate ($N_2H_4 \cdot H_2O$, 80%) is purchased from Xiya reagent. Ammonium sulfate ($(NH_4)_2SO_4$, ≥99.997%), sodium nitroferricyanide dihydrate ($Na_2Fe(CN)_5NO \cdot 2H_2O$, 99%), N-(-1-naphthyl) ethylenediamine dihydrochloride (NED, $C_{12}H_{14}N_2 \cdot 2HCl$, 98%), and Deuterium dimethyl sulfoxide (DMSO, 99.9%) is purchased from Aladdin. Para-(dimethylamino) benzaldehyde (p-$C_9H_{11}NO$, 99%), bismuth acetate ($Bi(CH_3COO)_3$, 99.995%), and sodium nitrite ($NaNO_2$, 99.99%) are obtained from Innochem. Nafion D-521 dispersion (5% W/W) and Nafion-117 membrane are purchased from Dupont. Reduced graphene oxide powder (RGO, EFG-P001) is provided by Baotailong graphene New Material CO., Ltd. N_2 (99.999%) and Ar (99.999%) are purchased from the Beijing Qianxi Jingcheng Gas Co., Ltd. $^{15}N_2$ (Enrichment 99 atom% ^{15}N) is purchased from Wuhan Newradar. The purified water for this experiment is purchased from Hangzhou Wahaha Group Co. Ltd.

Characterizations: Shimadzu XRD-6000 powder diffractometer equipped with a Cu Kα source (λ=0.154) is used to collect the Wide-angle X-ray diffraction (XRD) patterns. The surface morphology and internal structure of all samples are observed on a ZEISS Gemini 300 scanning electron microscope (SEM) and Joel F200 transmission electron microscope (TEM), respectively. X-ray photoelectron spectroscopy (XPS) studies are performed on the Thermo Scientific K-Alpha. Calibration is carried out with surface contamination C 1s (284.8 eV) as the standard. Raman spectra of all the samples are recorded on a HORIBA Scientific LabRAM HR Evolution. Electron paramagnetic resonance (EPR) is taken to investigate the samples that contained unpaired electron on Bruker A300. Temperature programmed desorption (TPD) is conducted by AutoChem1 II 2920 to determine the N_2 absorption on the prepared materials.

Syntheses of the Bi-RGO: Typically, a mixture of RGO powder (40 mg) and $Bi(CH_3COO)_3$ (12 mg) is put into an agate mortar. After physically grinding for about 15 min, the mixture is transferred to an alumina crucible and then heated to 250 ℃ for 1.5 h in a tube furnace with a heating rate of 10 ℃/min in the Ar atmosphere. The Bi-RGO is obtained after natural cooling. The reaction during the heat treatment is: (1) $Bi(CH_3COO)_3 + RGO \rightarrow Bi + CO_2 + CO + H_2O + RGO$.

Syntheses of the odBi-hRGO: Briefly, the obtained Bi-RGO is put into an alumina crucible and heated to 250 ℃ for 3 h in a muffle furnace with a heating rate of 10 ℃/min in the air atmosphere. The obtained Bi_2O_3-RGO is then naturally cooled down to room temperature. After that, it is transferred to a tube furnace and then heated to 400 ℃ for 1h with a heating rate of 10 ℃/min in the Ar atmosphere. Finally, the odBi-hRGO is obtained after natural cooling. The reaction equations are: (2) $Bi + RGO + O_2 \rightarrow Bi_2O_3 + RGO$ and (3) $Bi_2O_3 + RGO \rightarrow Bi + hRGO$.

Electrochemical measurements: An H-type electrolytic cell with two compartments that are separated by nafion117 membrane is employed to evaluate the NRR performance in N_2- or Ar-saturated 0.05 M H_2SO_4 electrolyte at ambient conditions. For the preparation of the cathode electrode, 2 mg of odBi-dG is dispersed in 1 mL of the aqueous solution containing 0.9 mL ethanol, and 0.1 mL Nafion by ultrasonic for 10 min to form the uniform ink. 10 μL of ink is then loaded onto the L-type glass carbon electrode (GCE) with a diameter of 0.5 cm (sample loading: ~0.1 mg cm^{-2}) and dried under natural conditions. Ag/AgCl electrode saturated with KCl solution and platinum mesh electrode (1 cm×1 cm) serve as the reference electrode and counter electrode, respectively. Before NRR tests, the Nafion membrane is rigorously cleaned according to the report by Hanifpour *et al.*[S1] Besides, N_2 is filtered in advance through a gas-washing cell containing 0.05 M H_2SO_4 and then bubbled into the cathode chamber for 30 minutes under magnetic stir. According to the Nernst equation, all potentials reported are converted to the reversible hydrogen electrode (RHE) by adding a value of (0.059pH+0.197) V in this work.

Quantification of $^{14}NH_4^+$ *via* the indophenol blue method: 2 mL H_2SO_4 (0.05 mol/L)

containing known $(NH_4)_2SO_4$ concentration solution is added into 2 mL NaOH (1 mol/L) of stock solution containing salicylic acid (5 wt%) and sodium citrate (5 wt%) in a serum bottle. Subsequently, 1 mL of 0.05 M NaClO and 0.2 mL of $Na_2Fe(CN)_5NO$ (1 wt.%) are added into the above solution in turn. After standing at ambient conditions for 2 h, 2.6 mL mixture is transferred to colorimeter tube and the absorption spectrum is determined using an ultraviolet-visible (UV-vis, Shimadzu 8000) spectrophotometer. The standard curve can be constructed by measuring the ammonia signal that appeared at the wavelength of 655 nm as a function of the known $(NH_4)_2SO_4$ standard solution.

Quantification of $^{14}NH_4^+$ *via* ^{1}H NMR: 0.03 mL DMSO-d6 (internal standard) is added into 0.57 mL H_2SO_4 (0.05 mol/L) containing known $(NH_4)_2SO_4$ concentration solution in a nuclear magnetic tube and the ^{1}H NMR spectrum is determined on the Bruker Advance III 400. The standard curve can be constructed by integrating the ammonia signal that appeared at 6.93 ppm as a function of the known $(NH_4)_2SO_4$ standard solution. To determine the NH_3 yield of the odBi-hRGO, after 2h electrolysis at -0.6 V, 10 mL of the electrolyte is taken out and concentrated to ~1 mL at 70 ℃ *via* reduced pressure distillation. 0.57 mL of the resulting electrolyte is taken out and mixed with 0.03 mL DMSO-d6 for 1H-NMR measurement.

$^{15}N_2$ isotope labeling experiments: The reaction cell is first repeatedly purged with Ar for three times to remove residual N_2 and O_2. The $^{15}N_2$ is then bubbled into the electrolyte with the injection rate of ~50 mL every 10 min. After 4h electrolysis at -0.6 V, 30 mL of the electrolyte is taken out and then concentrated to ~1 mL at 70 ℃ *via* reduced pressure distillation. Similarly, we still use NMR to detect the products, of which a known amount of $^{15}NH_4Cl$ (^{15}N: 10 atom%) is used as a reference.

Quantification of hydrazine: Generally, hydrazine as the by-product is determined by the method of Watt and Chrisp. Briefly, 6.05 g of p-$C_9H_{11}NO$, 30 mL of concentrated HCl, and 300 mL of absolute ethanol are first added in a 500 mL volumetric flask as the hydrazine chromogenic agent. Subsequently, 2 mL of hydrazine chromogenic agent and 2 mL H_2SO_4 (0.05 mol/L) containing known hydrazine concentration solution are added into a serum bottle. After standing at ambient conditions for 10 min, 2 mL mixture is transferred to colorimeter tube and the absorption spectrum is determined

using a UV-vis spectrophotometer. The standard curve can be constructed by measuring the hydrazine signal that appeared at the wavelength of 455 nm as a function of known hydrazine standard solution.

Quantification of NO_x: N-(-1-naphthyl) ethylenediamine dihydrochloride (NED) spectrophotometric method is employed to detect the NO_x. 25 mg NED, 2.5 g sulfanilic acid, and 25 mL acetic acid are dissolved in 500 mL H_2O as the NO_x chromogenic agent. Subsequently, 4 mL of NO_x chromogenic agent and 1 mL H_2SO_4 (0.05 mol/L) containing known $NaNO_2$ concentration solution is added into a serum bottle. After standing at ambient conditions for 10 min, 2.5 mL mixture is transferred to colorimeter tube and the absorption spectrum is determined using the UV-vis spectrophotometer. The standard curve can be constructed by measuring the hydrazine signal that appeared at a wavelength of 550 nm as a function of known hydrazine standard solution.

NH_3 Faradic efficiency (FE) and yield rate (YR): The NH_3 Faradic efficiency for NNR is defined as the electric charge used for generating ammonia divided by the total integral electric charge (Q) passed through the working electrodes within a certain reduction time. The FE is calculated using the equation as follows: $FE = 3 \times (C_{NH3} \times V / M) \times F / Q$, where "3" means three electrons are needed to produce one NH_3 molecule, C_{NH3} is the detected NH_3 concentration (μg mL^{-1}), V is the volume of electrolyte (mL), M is the molar mass of ammonia (17 g mol^{-1}), F is the Faraday constant (96485 C mol^{-1}), and $Q = \int_0^t I\mathrm{d}t$. The yield rate of NH_3 can be obtained as follows: $YR = (C_{NH3} \times V) / (t \times S)$, where t is the reduction time (h) and S is the catalyst loading area (cm^2).

Calculation method: Density functional theory (DFT) calculations are performed using the Vienna Ab Initio Simulation Package (VASP) for the optimization of atomic structures of the odBi-hRGO.[S2,S3] The generalized gradient approximation of Perdew, Burke, and Ernzerhof (PBE) is used to represent the exchange-correlation energy,[S4] and the projector-augmented wave (PAW) method with a 450 eV energy cutoff is used to describe the wave functions of the atomic cores.[S5,S6] The Brillouin zone is set to 3×3×1 Monkhorst-Pack k-point mesh. The slab used to represent the hRGO consists of 126 carbon atoms with a

divacancy at the center. Motivated by the magic atom numbers (13, 55, 147, etc.) of nanoclusters which provide a higher structural stability compared to other atom numbers, a nanoparticle consisting of 55 Bi atoms is modeled to represent the odBi (Bi_{55}). The size of the Bi_{55} nanoparticle is smaller than those Bi particles we have observed in the experiments, however, modeling larger Bi nanoparticles by DFT calculations is very demanding and the global optimization is hardly feasible. Considering the limitation of DFT calculations, we believe Bi_{55} is adequately large to represent the Bi catalyst. The isolated Bi_{55} nanoparticle is optimized in a 25 Å cubic supercell in which the Brillouin zone integration is conducted with the Γ-point only. To avoid the artificial iteration, the odBi-hRGO system is separated from its periodic images in the z-direction by a vacuum space of 20 Å. Geometries are optimized until the energy had converged to 1.0×10^{-5} eV per atom and the force converged to 0.01 eV/Å.

The adsorption energy is calculated using the following equation:

$$E_{ad} = E_{(sp+slab)} - (E_{sp} + E_{slab})$$

where E_{sp} , $E_{slab,}$ and $E_{(sp+slab)}$ are the total energies for the isolated species (e.g., N_2), the clean substrate (e.g., odBi-hRGO), and the substrate with the adsorbed species, respectively.

The Gibbs free energy (ΔG) is calculated as:

$$\Delta G = \Delta E + \Delta E_{ZPE} - T\Delta S$$

where ΔE is the total energy change obtained from DFT calculations, ΔE_{ZPE} is the change in zero-point energy, and ΔS is the change in entropy.

The climbing-image nudged elastic band (CI-NEB) method is used for reaction barrier calculations.[S7,S8]

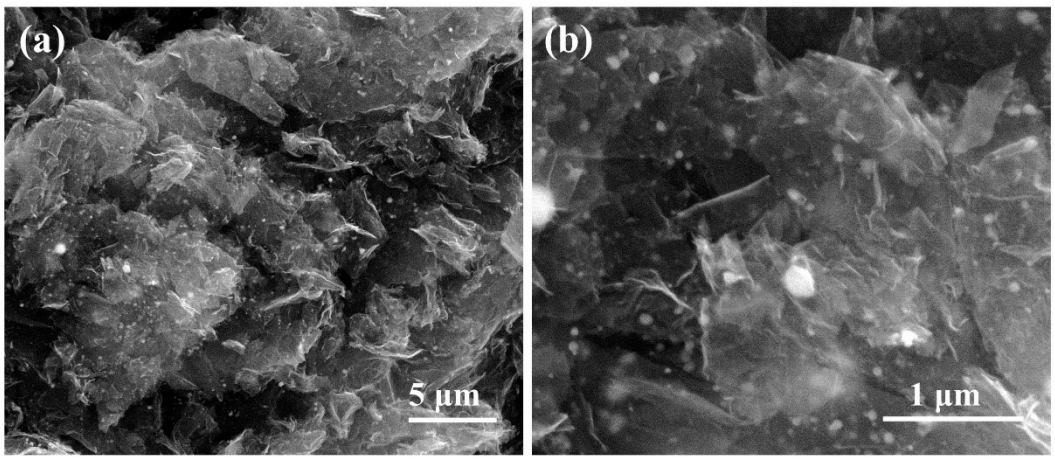

Figure S1. SEM images of the Bi-RGO sample.

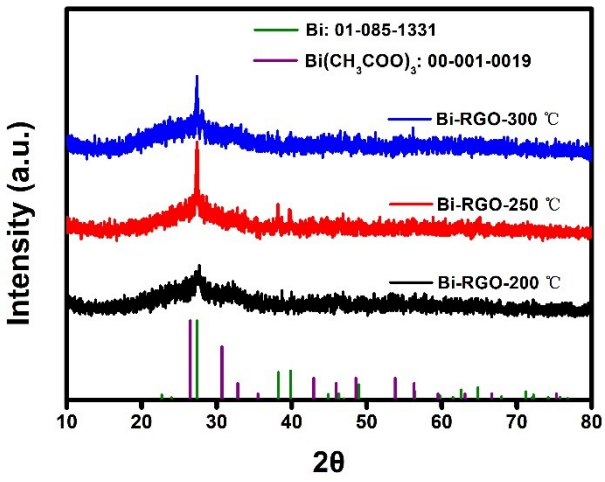

Figure S2. XRD patterns of the obtained Bi-RGO samples under various temperatures.

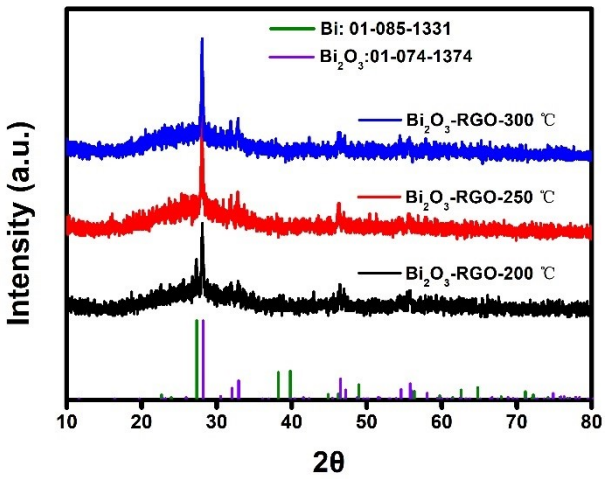

Figure S3. XRD patterns of the obtained Bi_2O_3-RGO samples under various temperatures.

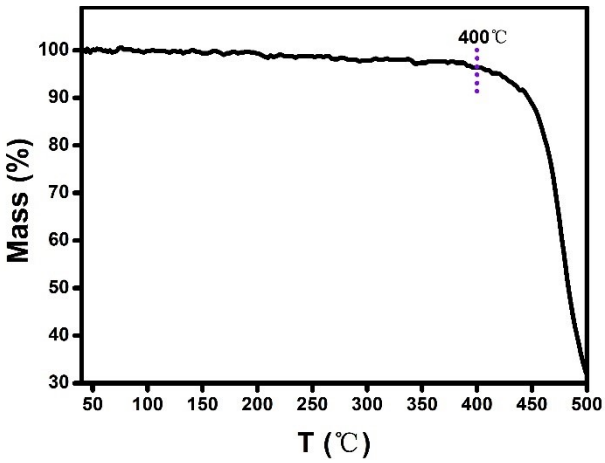

Figure S4. TGA data of the RGO in the air atmosphere.

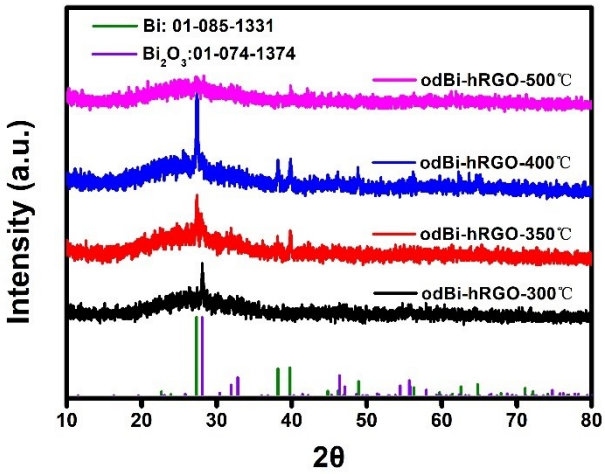

Figure S5. XRD patterns of the obtained odBi-hRGO samples under various temperatures.

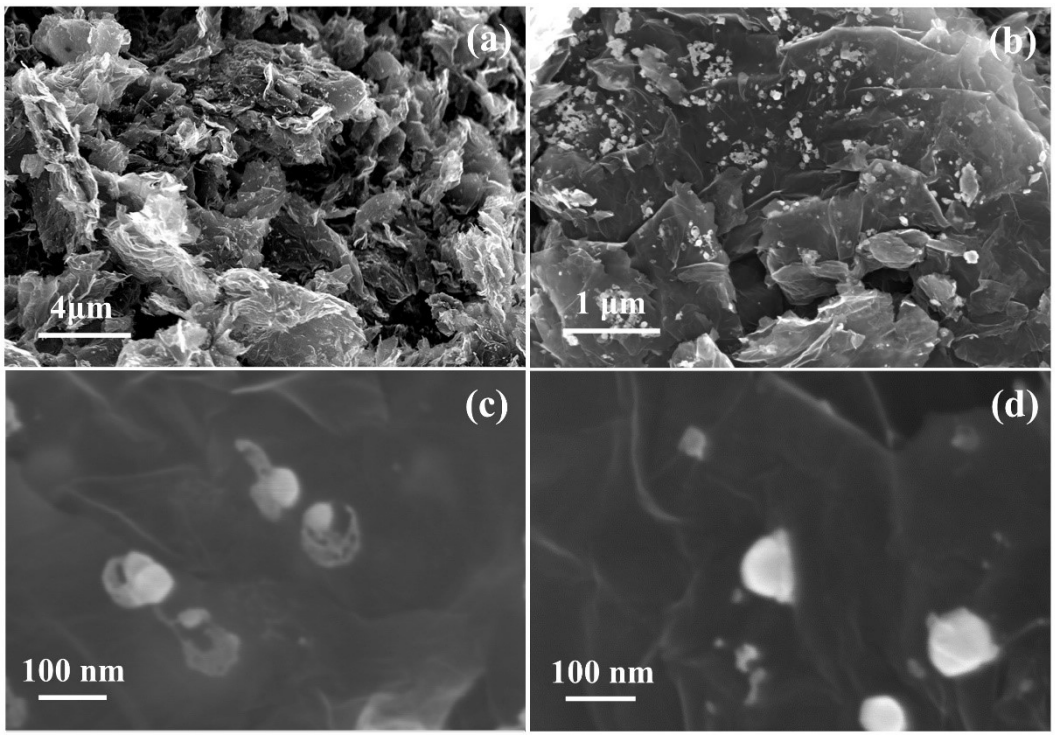

Figure S6. SEM images of the odBi-hRGO sample at different degrees of magnification.

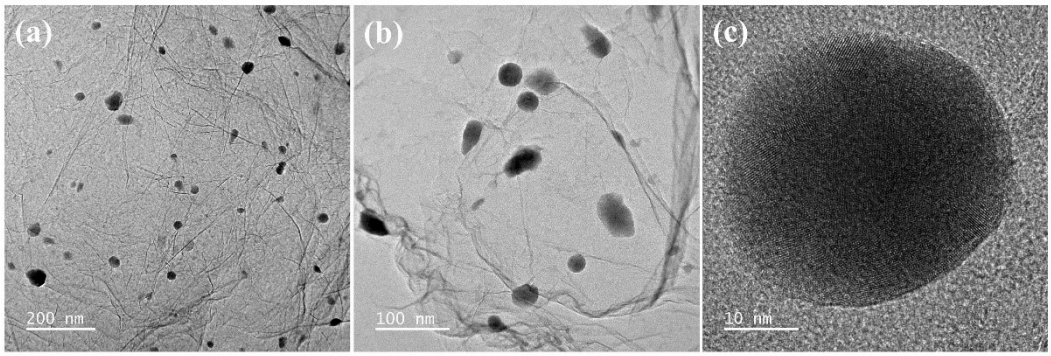

Figure S7. TEM images of the Bi-RGO sample at different degrees of magnification.

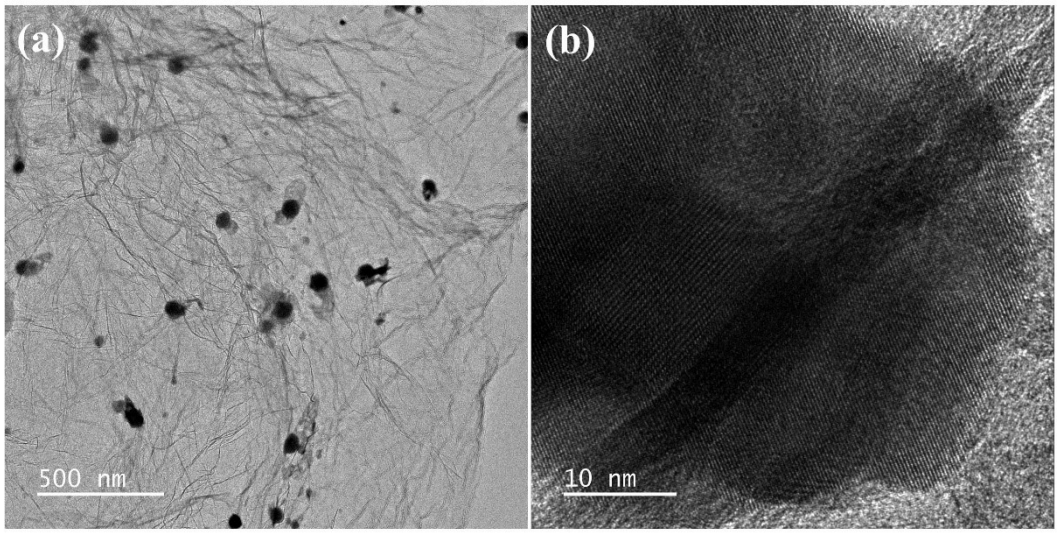

Figure S8. (a) TEM image and (b) cross-sectional HRTEM image of the odBi-hRGO sample.

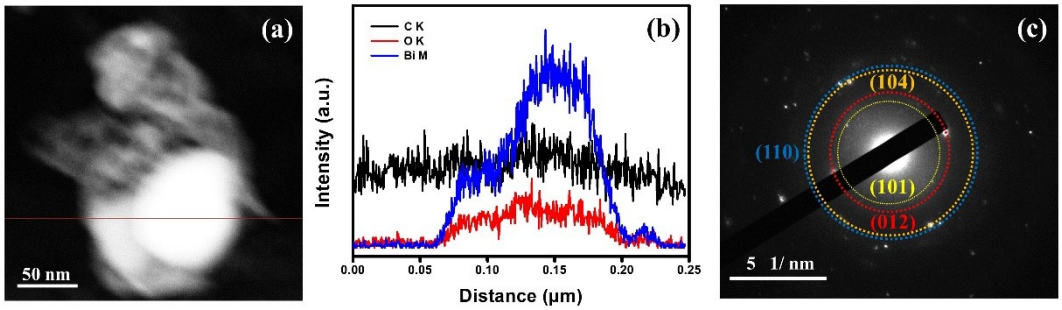

Figure S9. (a) Dark-field TEM image of the odBi-hRGO sample, (b) the corresponding elemental linear distribution, and (c) diffraction fringes.

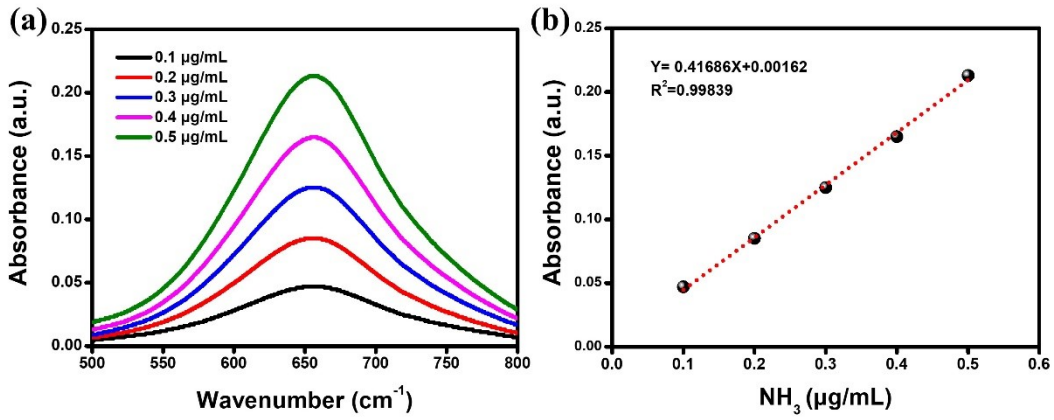

Figure S10. (a) UV-Vis absorption spectra of indophenol assays at different NH_3 concentrations incubated for 2 h and (b) calibration curve used for calculation of NH_3 concentrations.

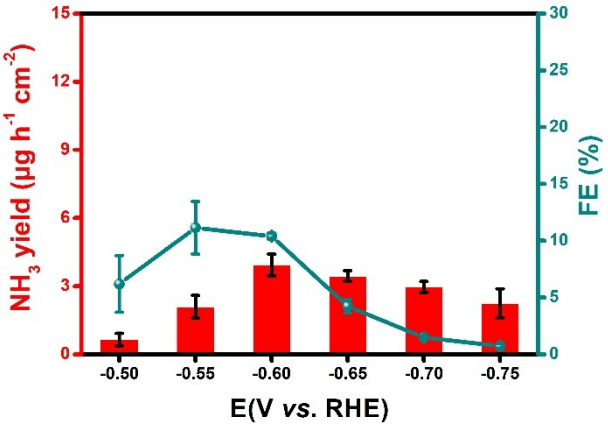

Figure S11. NH_3 yield and Faraday efficiency results of Bi-RGO.

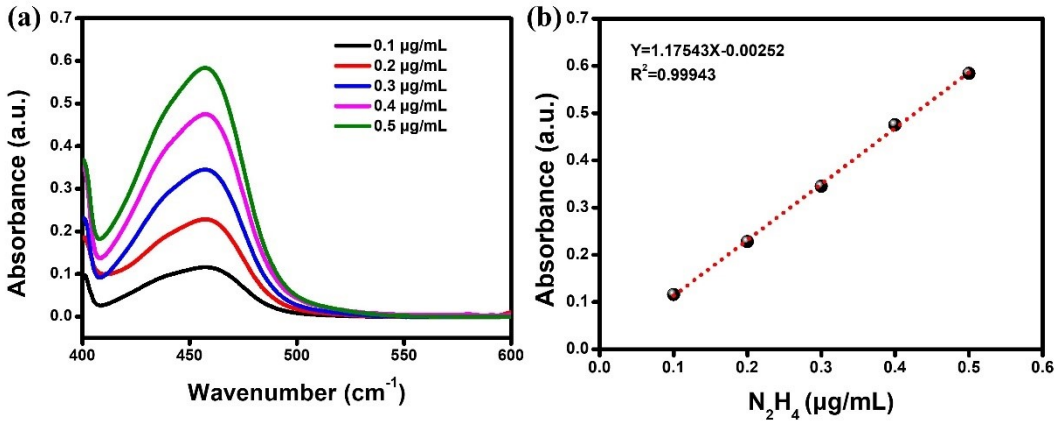

Figure S12. (a) UV-Vis absorption spectra of different N_2H_4 concentrations after incubated for 20 min stained with p-$C_9H_{11}NO$ indicator and (b) calibration curve used for calculation of N_2H_4 concentrations.

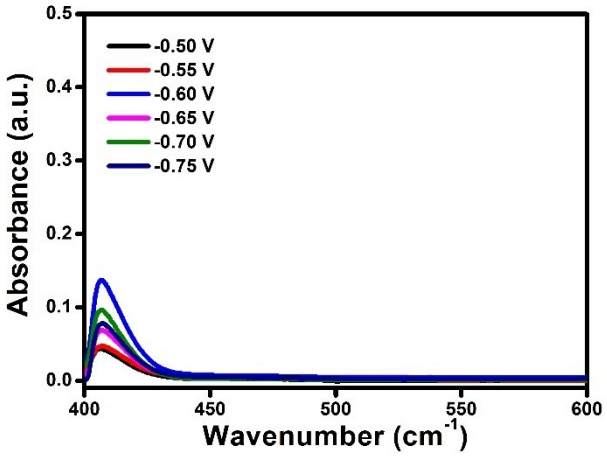

Figure S13. UV-Vis absorption spectra of the electrolytes stained with the p-$C_9H_{11}NO$ indicator for odBi-RGO at various applied potentials.

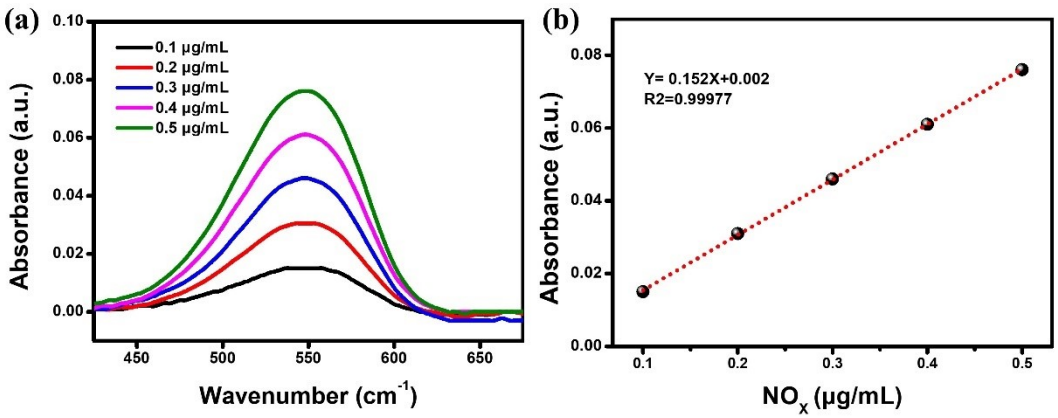

Figure S14. (a) The UV-vis absorption spectra and (b) corresponding calibration curves for the colorimetric NO_x using the NED spectrophotometric method in 0.05 M H_2SO_4.

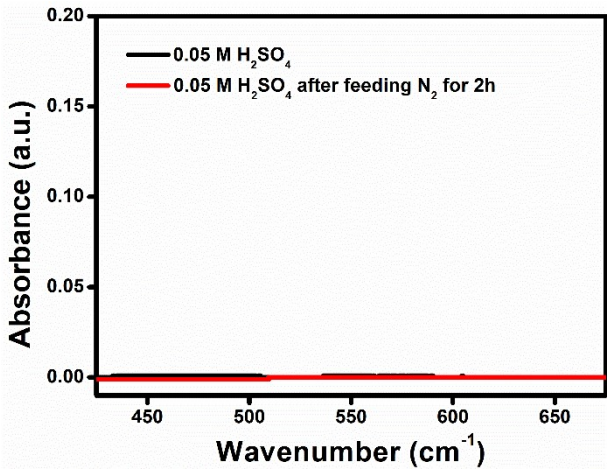

Figure S15. The UV-vis absorption spectra of the blank 0.05 M H_2SO_4 and the N_2-saturated 0.05 M H_2SO_4 solution.

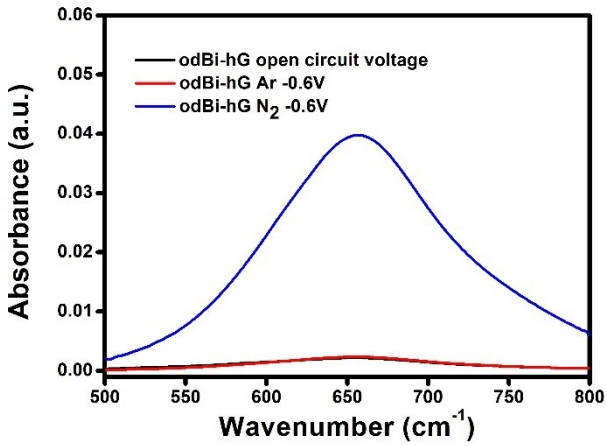

Figure S16. UV–vis absorption spectra of the electrolytes after 2 h electrolysis under various conditions.

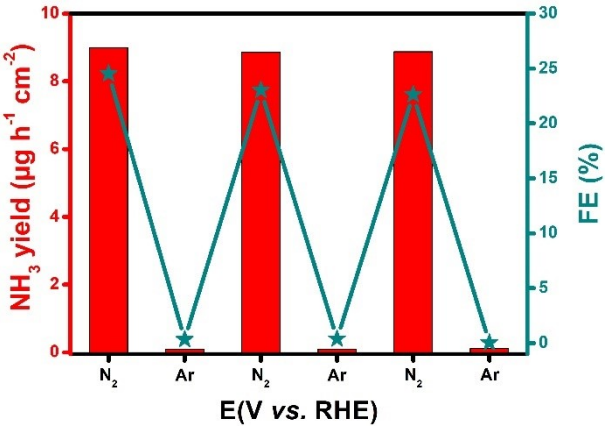

Figure S17. NH_3 yield and FE for odBi-hRGO at -0.6 V with alternating 2 h cycles between N_2- and Ar- saturated electrolytes.

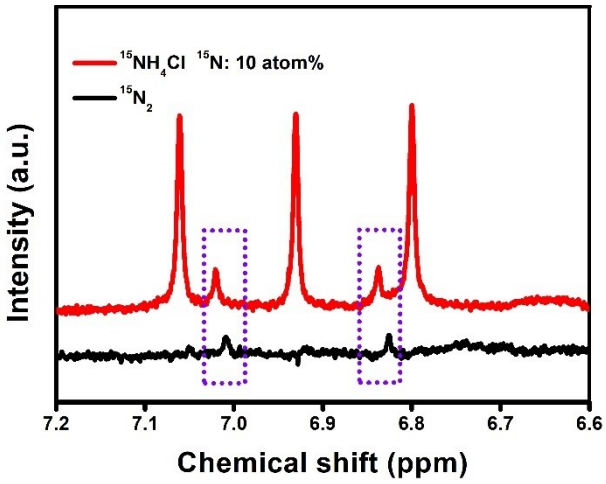

Figure S18. ^{1}H NMR spectra of $^{15}NH_4^+$ generated from $^{15}N_2$ electroreduction.

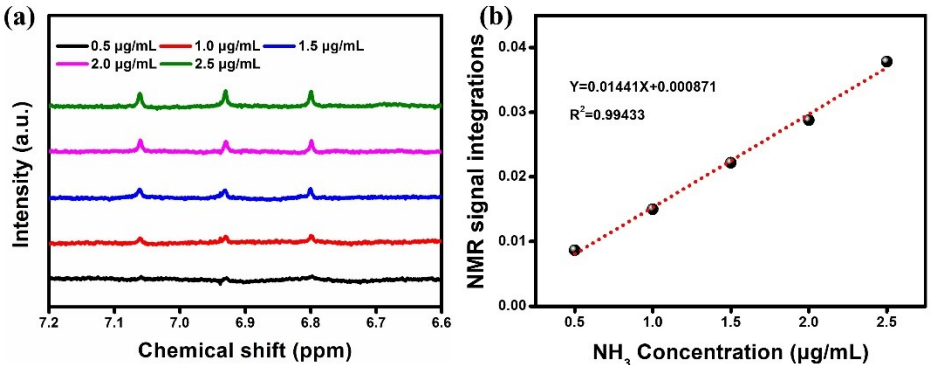

Figure S19. (a) ^{1}H NMR spectra of various $^{14}NH_3$ concentration. (b) Signal integral area ($^{14}NH_3$ / DMSO-d6) against $^{14}NH_3$ concentration.

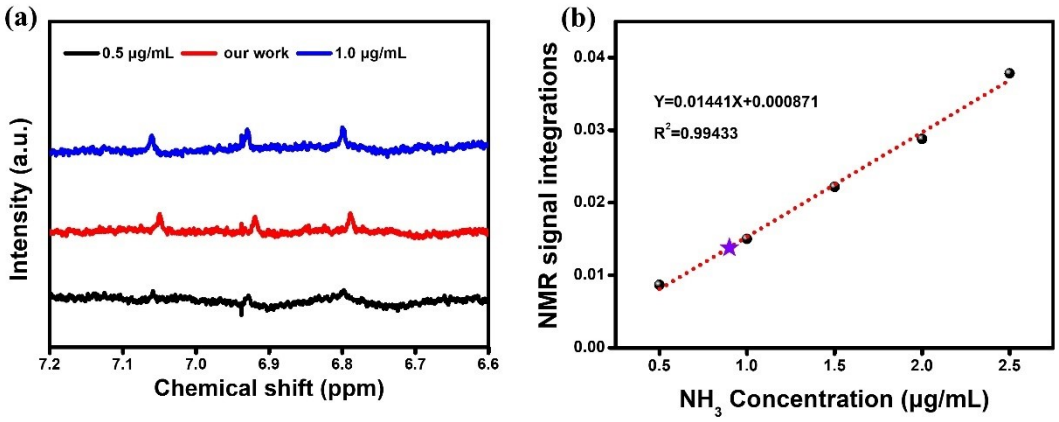

Figure S20. (a) ^{1}H NMR spectra of the electrolyte and the reference solution. (b) The $^{14}NH_3$ concentration of the electrolyte is quantitatively determined by ^{1}H NMR with external standards.

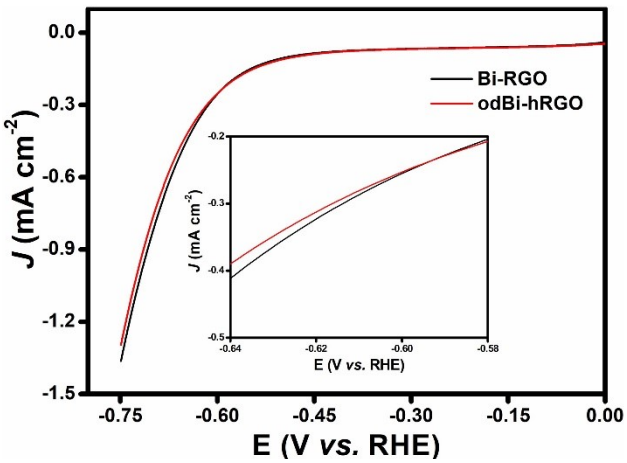

Figure S21. LSV curves of Bi-RGO and odBi-hRGO in Ar-saturated 0.05 M H_2SO_4 with a scan rate of 50 mV s^{-1}.

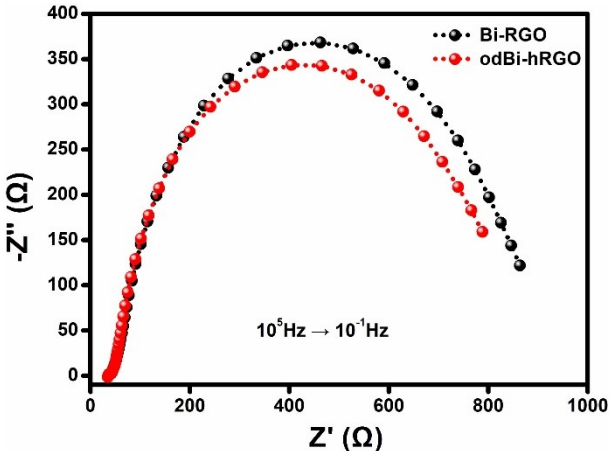

Figure S22. Nyquist plots of Bi-RGO and odBi-hRGO in N_2-saturated 0.05 M H_2SO_4 at -0.6V.

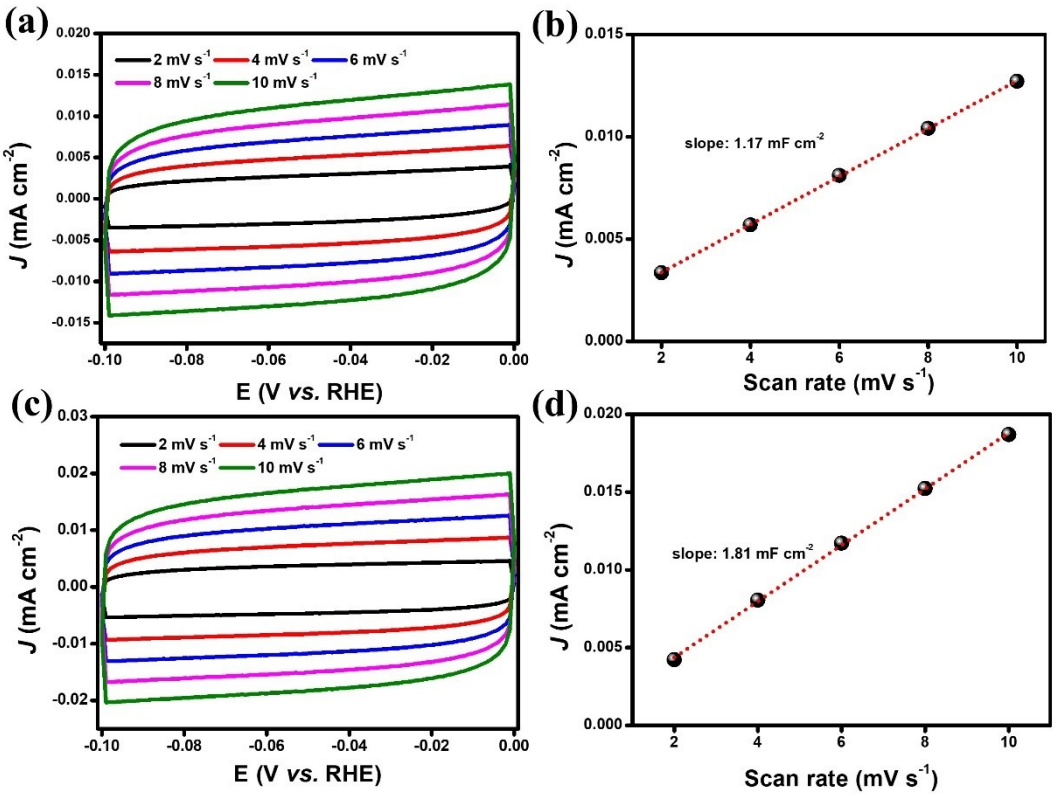

Figure S23. Measured cyclic voltammetry curves on (a) Bi-RGO and (c) odBi-hRGO with a potential range from -0.10 V to 0 V. The calculation of double-layer capacitances (C_{dl}) of (b) Bi-RGO and (d) odBi-hRGO. C_{dl} was obtained from the current density responses at -0.02 V against scan rates.

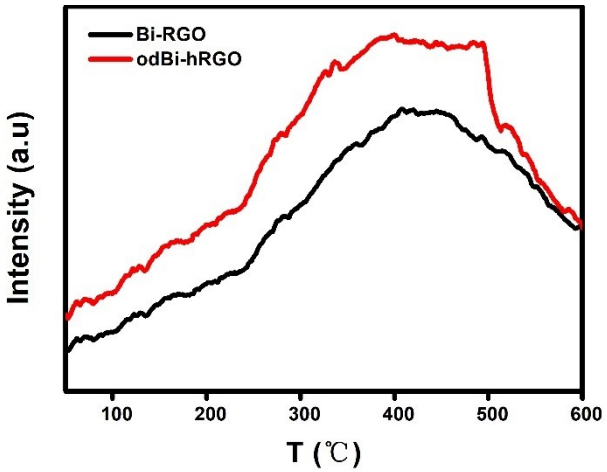

Figure S24. TPD test results of the Bi-RGO and odBi-hRGO samples.

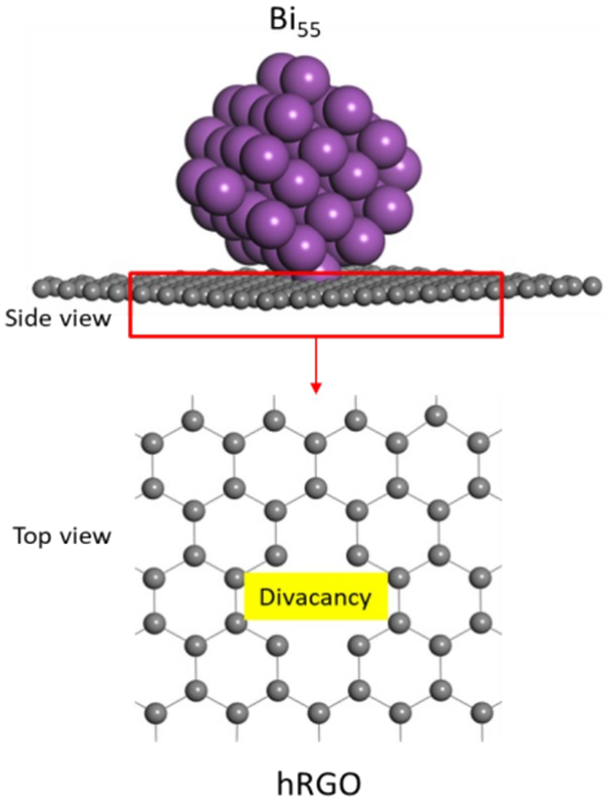

Figure S25. Schematic diagram of the oBi-hRGO model. Purple and grey colors represent Bi and C, respectively.

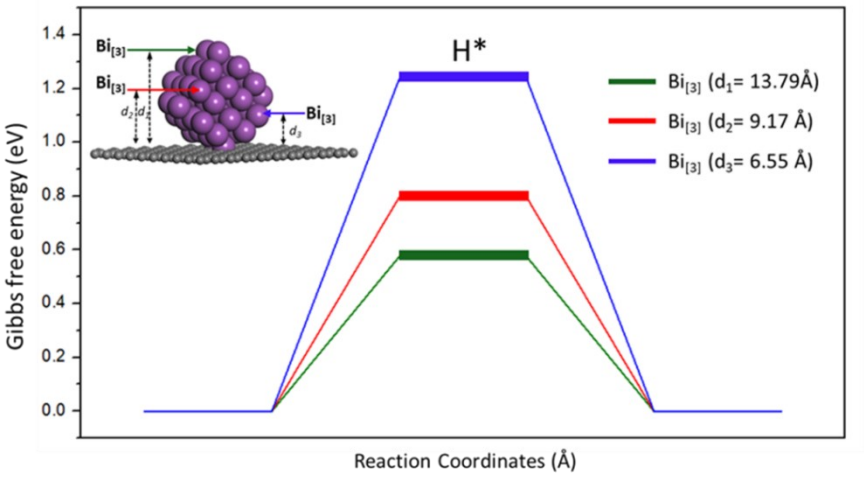

Figure S26. Gibbs free energy diagrams for HER on the various $Bi_{[3]}$ adsorption sites of the odBi-hRGO system.

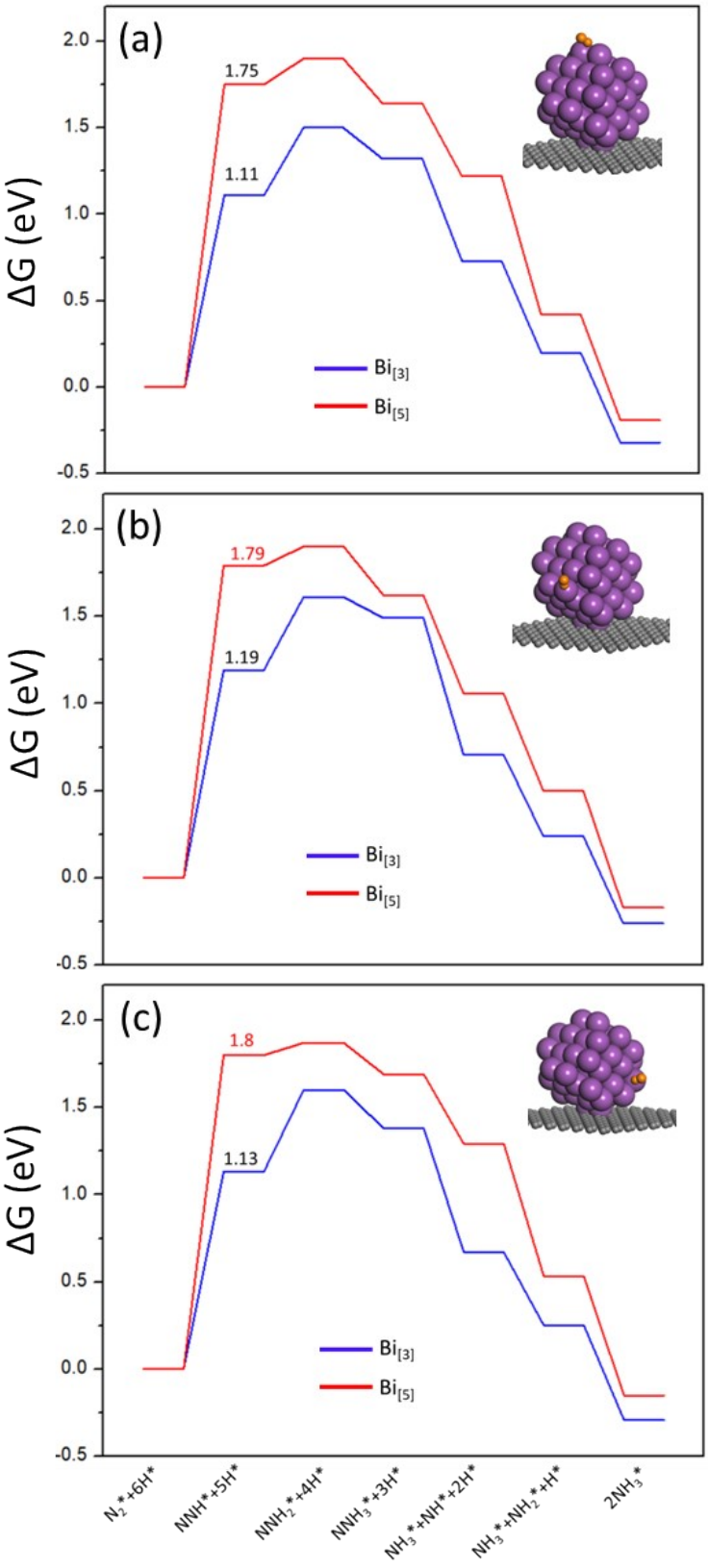

Figure S27. Gibbs free-energy diagram of the NRR on ideal Bi ($Bi_{[5]}$) and defective Bi ($Bi_{[3]}$) with the distance of (a) 13.79 Å, (b) 6.55 Å, and (c) 4.61 Å from the hRGO.

Table S1. A comparison of the reported Bi-based, defective RGO, and Sb electrocatalysts for NRR under ambient conditions.

Catalyst	**Electrolyte**	**YR (μg $h^{-1}cm^{-2}$)**	**FE (%)**	**Potential (V vs.RHE)**	**Ref.**
odBi-hRGO	0.05 M H_2SO_4	8.89	24.34	-0.6 for YR -0.55 for FE	This work
Bi nanosheets	0.1 M Na_2SO_4	2.54	10.46	-0.8	[17]
Bi nanocrystals	acidic 0.5 M K_2SO_4 (pH= 3.5).	884	66	-0.6	[18]
defect-rich Bi (also oxide-derived)	0.2 M Na_2SO_4	5.453	11.68	-0.9 for YR -0.6 for FE	[19]
BiNi Alloy	0.1 M Na_2SO_4	8.75	13.8	-0.6	[20]
Bi nanoparticles	0.1 M Na_2SO_4	3.25	12.11	-0.7 for YR -0.6 for FE	[21]
RGO with defects	0.1 M HCl	7.8	22	-0.116	[24]
Porous Bi electrode	0.5M phosphate buffer + 25 mM V_2O_5	unavailable	13.2	-0.2	[31]
Bi nanodendrites	0.1 M HCl	2.586	10.8	-0.6 for YR -0.55 for FE	[S9]
Bi nanosheet array	0.1 M HCl	4.22	10.26	-0.5	[S10]
Bi nanoparticles in carbon nanosheets	0.1 M Na_2SO_4	4.2	15.1	-0.6 for YR -0.4 for FE	[S11]
Bi nanoparticles on nickel foam	0.1 M Na_2SO4	5.6916	6.8	-0.5 for YR -0.475 for FE	[S12]
nanoporous Sb	0.1 M KOH	2.3	45	-0.3 for YR -0.1 for FE	[S13]

Supplemental References

S1 F. Hanifpour, A. Sveinbjörnsson, C. P. Canales, E. Skulason, H. D. Flosadóttir, *Angew. Chem. Int. Ed.* 2020, **132**(51), 23138-23142.

S2 G. Kresse, J. Furthmüller, *Comput, Mater. Sci.* 1996, **6**, 15-50.

S3 G. Kresse, J. Furthmüller, *Phys. Rev. B.* 1996, **54**, 11169.

S4 J. P. Perdew, K. Burke, M. Ernzerhof, *Phys. Rev, Lett.* 1996, **77**, 3865.

S5 P. E. Blöchl, *Phys. Rev. B.* 1994, **50**, 17953.

S6 G. Kresse, D. Joubert, *Phys. Rev. B.* 1999, **59**, 1758-1775.

S7 G. Henkelman, B. P. Uberuaga, H. Jónsson, *J. Chem. Phys.* 2000, **113**(22), 9901–9904.

S8 G. Henkelman, H. Jónsson, *J. Chem. Phys.* 2000, **113**(22), 9978–9985.

S9 F. Wang, X. Lv, X. Zhu, J. Du, S. Lu, A. A. Alshehri, K. A. Alzahrani, B. Zheng and X. Sun, *Chem. Commun.* 2020**, 56** (14), 2107-2110.

S10 R. Zhang, L. Ji, W. Kong, H. Wang, R. Zhao, H. Chen, T. Li, B. Li, Y. Luo and X. Sun, *Chem. Commun.* 2019**, 55** (36), 5263-5266.

S11 Y. C. Wan, H. Z, M. Y. Zheng, Z. H. Huang, F. Y. Kang, J. Li and R. T. Lv, *Adv. Funct. Mater.* 2021**,** *2100300*.

S12 G. Li, Z. Pan, H. Lin and L. An, *J. Alloys Compd.* 2021**, 875**, 160006.

S13 G. Fan, W. Xu, J. Li, J. L. Chen, M. Yu, Y. Ni, S. Zhu, X. C. Su and F. Cheng, *Adv. Mater.* 2021**, 33** (42), e2101126.